

# Domain Wall Network: A Dual Solution for Gravitational Waves and Hubble Tension?

Ligong Bian,<sup>1,2,\*</sup> Shuailiang Ge,<sup>2,3,†</sup> Changhong Li,<sup>4</sup> Jing Shu,<sup>3,2,5,‡</sup> and Junchao Zong<sup>6,7</sup>

<sup>1</sup>Department of Physics and Chongqing Key Laboratory for Strongly Coupled Physics, Chongqing University, Chongqing 401331, China

<sup>2</sup>Center for High Energy Physics, Peking University, Beijing 100871, China

<sup>3</sup>School of Physics and State Key Laboratory of Nuclear Physics and Technology, Peking University, Beijing 100871, China

<sup>4</sup>Department of Astronomy, Key Laboratory of Astroparticle Physics of Yunnan Province, School of Physics and Astronomy, Yunnan University, No.2 Cuihu North Road, Kunming, 650091 China

<sup>5</sup>Beijing Laser Acceleration Innovation Center, Huairou, Beijing, 101400, China

<sup>6</sup>Department of Physics, Nanjing University, Nanjing 210093, China

<sup>7</sup>CAS Key Laboratory of Theoretical Physics, Institute of Theoretical Physics, Chinese Academy of Sciences, Beijing 100190, China

We search for stochastic gravitational wave background (SGWB) generated by domain wall networks in the Data Release-2 of Parkes Pulsar Timing Array and find that the observed strong common power-law process can be explained by domain wall networks for the wall tension  $\sigma_{\text{DW}} \sim (29 - 414 \text{ TeV})^3$  and the wall-decay temperature  $T_d \sim 20 - 257 \text{ MeV}$  at 68% Credible Level. Interestingly, the same parameter region can largely alleviate the Hubble tension, if the free particles generated from domain wall networks further decay into dark radiation. This coincidence that a domain wall network can simultaneously account for the nano-Hertz SGWB and Hubble tension is robust, independent of domain wall parameters and applicable to observations by other pulsar timing array collaborations in general. On the other hand, assuming that the common power-law process is not due to domain wall networks, we can put stringent constraints on the wall tension and decay temperature.

**Introduction.** A Domain Wall (DW) is a two-dimensional topological defect, forming as a field connects discrete vacua, possibly manifesting during the Universe's early phase transition through the Kibble-Zurek mechanism [1, 2][69]. The dynamics of a DW network have nonzero quadrupole momentum and thus can generate gravitational waves (GWs) [3–5], but their slower dilution compared to matter and radiation can dominate the universe's energy density, posing the Domain Wall problem [6]. The application of a biased potential can rapidly decay these walls, thereby marking the cessation of GW production [7–9]. The domain wall tension and the biased potential influence the magnitude and peak-frequency position of the resultant GW spectrum.

The Stochastic GW Background (SGWB) generated by DW networks falls within the detection range of Pulsar Timing Array (PTA) experiments for certain parameters. PTAs, designed to monitor millisecond pulsars with precise Time of Arrivals, have discovered a common power-law (CPL) process in the analysis of NANOGrav 12.5-year data [10], further confirmed by other PTA collaborations such as Parkes Pulsar Timing Array (PPTA) [11] and European Pulsar Timing Array (EPTA) [12]. This CPL signal, while encouraging as potential first light of GW detection via PTAs, necessitates further observation of the “Hellings-Downs” (HD) correlation for a definitive GW explanation [13]. The signal's origin remains elusive, with investigations into various sources such as supermassive black hole binaries, first-order phase transitions, and cosmic strings [14–19]. The SGWB induced by domain walls shows a broken power-law shape, distinguishing it from the wide-frequency-range plateau shape exhibited by cosmic strings.

Besides decaying into GWs, most DW network energy is released as free particles. In this Letter, one intriguing observation is that the free particles can significantly alleviate the Hubble tension if assuming they can further decay into

dark radiation. Here the Hubble tension refers to the  $4.1\sigma$  conflict between the values of the current Hubble constant derived from the early Universe measurements [20] and from the local late Universe measurements [21]. Remarkably, the same parameter space accounting for the CPL process can simultaneously alleviate the Hubble tension from a stark  $4.1\sigma$  to a more reconcilable  $2.7\sigma$ . Such a coincidence is very robust, as the proportions decaying into GWs and dark radiation remain fixed independent of the DW's specific properties. This coincidence holds true in general attempts of using a DW network to explain the potential SGWB, and it applies to the observation datasets from various PTA collaborations [10–12, 22–26].

Specifically, in this Letter, we utilize the second dataset released by Parkes PTA (PPTA) to probe a potential SGWB signal [27]. The DW tension and the decay temperature are considered as two free parameters in our search for corresponding GW signals. We ascertain that specific parameter space of the DW network can account for the CPL process observed in the PPTA data, and the observed Hubble tension can be substantially alleviated by the concurrent production of dark radiation. This finding could serve as an essential hint towards a DW network's existence in the early Universe. Alternatively, if we consider the CPL process as an unknown background unrelated to a DW network, we can establish stringent constraints on DW parameters accordingly.

**SGWB spectra from DW networks.** The interaction between DWs is so efficient that their density after its formation will soon saturate the requirement of causality, i.e., approximately one piece of DW per Hubble patch  $H^{-3}$ . The energy density of DW networks thus evolves with the scaling behavior  $\rho_{\text{DW}}(t) \propto H(t)$ , which has been found and confirmed in multiple numerical simulations [4, 5, 28–31]. The DW density is  $\rho_{\text{DW}} = \mathcal{A}\sigma_{\text{DW}}H$  where  $\sigma_{\text{DW}}$  is the wall tension and  $\mathcal{A}$  is the area parameter. DW networks radiate GWs with the power  $P_{\text{GW}} \sim G\ddot{Q}_{ij}\ddot{Q}_{ij}$  where  $Q_{ij} \sim \mathcal{A}\sigma_{\text{DW}}H^{-4}$  is the quadrupole

momentum of the walls. Then the energy density of GWs can be expressed as  $\rho_{\text{GW}} = \epsilon P_{\text{GW}} t / H^{-3} = \epsilon G \mathcal{A}^2 \sigma_{\text{DW}}^2$  where an efficiency parameter  $\epsilon$  is introduced.  $\mathcal{A}$  and  $\epsilon$  are constant with time in the scaling regime and can be determined by numerical simulations [4, 5].

To avoid the DW domination problem, we introduce a biased potential  $\Delta V$  to quickly kill the networks [7–9] by breaking the degeneracy of vacua on the two sides of a wall. Such wall decay happens at  $H^{-1}(T_d) \simeq \sigma_{\text{DW}} / \Delta V$  when the biased potential energy of a vacuum patch is comparable with the energy of boundary wall. This is the time that the GW radiation stops, which determines the peak frequency of the GW spectra,  $f_p(T_d) \simeq H(T_d)$  [4, 5]. We assume that  $T_d$  is in the radiation-dominant era. Then, the peak frequency today is

$$f_p(T_0) \simeq 1.13 \times 10^{-8} \text{ Hz} \cdot \left[ \frac{g_*(T_d)}{10.75} \right]^{1/6} \left( \frac{T_d}{100 \text{ MeV}} \right). \quad (1)$$

where  $g_*$  is the effective degrees of freedom for energy. We then define the GW spectra as

$$\Omega_{\text{GW}}(f, T) \equiv \frac{1}{\rho_c} \frac{d\rho_{\text{GW}}(f, T)}{d \ln f}, \quad (2)$$

where  $\rho_c = 3H^2/(8\pi G)$  is the critical density. The present GW spectra at peak frequency is thus

$$\begin{aligned} \Omega_{\text{GW}}(f_p, T_0) h^2 \\ \simeq 6.5 \times 10^{-10} \mathcal{A}^2 \tilde{\epsilon} \cdot \left[ \frac{10.75}{g_*(T_d)} \right]^{4/3} \left( \frac{\sigma_{\text{DW}}}{10^6 \text{ TeV}^3} \right)^2 \left( \frac{100 \text{ MeV}}{T_d} \right)^4. \end{aligned} \quad (3)$$

where  $\tilde{\epsilon} \equiv [d\epsilon/d \ln f]_{f=f_p}$ .

As known, the spectra of  $f < f_p$  goes as  $\sim f^3$  because of causality [32, 33]. For  $f > f_p$ , simulations show that the slope is close to  $\sim f^{-1}$  but only slightly depends on the “domain wall number”  $N_{\text{DW}}$  which is the number of vacua [4, 5]. We consider scenarios of  $N_{\text{DW}} \geq 2$  since the  $N_{\text{DW}} = 1$  string-wall network is unstable and would disappear immediately after their formation without significant GWs production [34]. In the main text, we take  $\Omega_{\text{GW}}(f, T_0) h^2 = \Omega_{\text{GW}}(f_p, T_0) h^2 \times (f/f_p)^{-1.077}$  for  $f > f_p$  and present the result of the scenario  $N_{\text{DW}} = 2$ . For other scenarios with different  $N_{\text{DW}}$ , see *supplemental material* for details.

Throughout this work, we take the parameters  $\mathcal{A} = 1.2$ ,  $\tilde{\epsilon} = 0.7$  [4, 5] and fix  $g_*(T_d)$  at 10.75. In Fig. 1, we show the GW spectra for various values of  $\sigma_{\text{DW}}$  and  $\Delta V$ , in comparison with the free-spectra searching results for the SGWB amplitude using the PPTA dataset (2nd release). This plot tells the rough region of DW parameters that the PPTA data is sensitive to. We are going to carry out detailed data analysis in the following sections.

**Data analysis.** Our analysis employs the second data release of the PPTA data. We adhere to the standard procedure, using the TEMPO2 tool [35, 36] to fit for the timing model of the pulsar arrays, along with the ENTERPRISE [70], ENTERPRISE EXTENSIONS [71], and PTMCMCSampler [37]

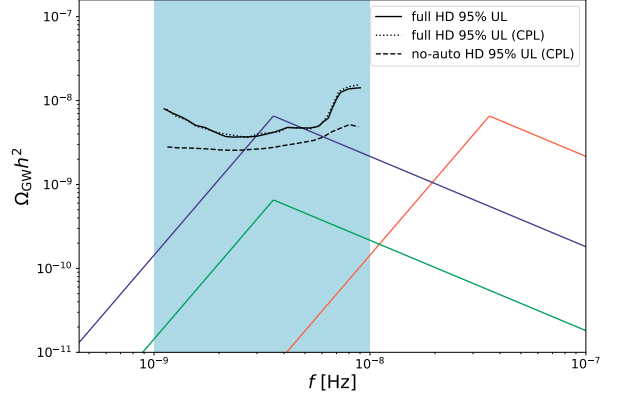


FIG. 1: The 95% upper limit (U.L.) on the SGWB amplitude by searching the 2nd released PPTA data. The shaded region indicates the PPTA-sensitive frequency range. The black solid, dotted, and dashed lines are the search results under different hypotheses H2/3/4 in Table I (but with the DW spectra replaced by the free spectra in the corresponding hypotheses). We also show the GW spectra of  $N_{\text{DW}} = 2$  as an example with different values of  $(\log_{10} \sigma_{\text{DW}} / \text{GeV}^3, \log_{10} T_d / \text{GeV})$ : (16.5, -0.5) in red, (14.5, -1.5) in purple and (14.0, -1.5) in green for illustrative purpose.

packages for noise modeling and Bayesian analysis. The identification of the SGWB signal in PTA involves searching for the Hellings-Downs (HD) correlation of the time of arrivals (ToAs) for the pulsar array, which necessitates the removal of noise generated during observation. Generally, two types of noises need to be considered: red and white noises. Red noises can originate from irregular pulsar spin (spin noise) or dispersion measure noise of the pulse during transit through interstellar media. All types of red noise are modeled to have power-law spectra, parameterized by an amplitude  $A$ , and a power  $\gamma$ . We employ EFAC (Error FACtor) and EQUAD (Error added in QUADrature) to account for additional white noise from the correlation of ToAs across multiple frequency channels. This white noise includes ToA uncertainties and ECORR (Error of CORrelation between ToAs in a single epoch) that are not accounted for. In practice, these white noise parameters are fixed by their maximum-likelihood values obtained from single pulsar analysis, as they bear little relation to SGWB model parameters [38]. All the parameters and their priors used in the Bayesian analysis are summarized in Table S1 in the supplemental material, where we have also considered the constraints from e.g., big bang nucleosynthesis (BBN) to set the prior range of DW parameters.

Then, to extract signal information from posterior data, we adopt Bayesian analysis method here. We use the Bayes factor  $\text{BF}_{10}$  to measure the strength of the signal hypothesis  $H_1$  against the null hypothesis  $H_0$ , which is given by the Savage Dickey formula[39]

$$\text{BF}_{10} = \frac{P_1(\mathbf{D})}{P_0(\mathbf{D})} = \frac{P(\phi = \phi_0)}{P(\phi = \phi_0 | \mathbf{D})}, \quad (4)$$

TABLE I: Description of the hypotheses, Bayes factors, and parameters estimation of  $N_{\text{DW}} = 2$ . “—” in the column of Parameters Estimation represents for the parameter is absent in that hypothesis.

Hypothesis	Pulsar Noise	CPL	SMBHB	DW Spectra	Parameter Estimation (68% C.L.)		
					$\log_{10} T_d/\text{GeV}, \log_{10} \sigma_{\text{DW}}/\text{GeV}^3$	$A_{\text{CPL}}, \gamma_{\text{CPL}}, A_{\text{SMBHB}}$	Bayes Factors
H0	✓				—	—	—
H1	✓	✓			—	$-14.48^{+0.62}_{-0.64}, 3.34^{+1.37}_{-1.53}, —$	$10^{3.2}$ (/H0)
H2	✓			✓(full HD)	$-1.24^{+0.65}_{-0.47}, 14.60^{+2.25}_{-1.20}$		$10^{2.1}$ (/H0)
H3	✓	✓		✓(full HD)	$> -2.48, < 17.73$ (95% C.L.)	$-14.67^{+0.65}_{-0.98}, 3.42^{+1.47}_{-1.65}, —$	1.02 (/H1)
H4	✓	✓		✓(no-auto HD)	$> -2.57, < 17.75$ (95% C.L.)	$-13.62^{+0.14}_{-0.14}, 4.67^{+0.33}_{-0.32}, —$	0.89 (/H1)
H5	✓		✓		—	$—, —, -14.89^{+0.10}_{-0.12}$	$10^{3.3}$ (/H0)
H6	✓		✓	✓(full HD)	$> -1.04, < 16.45$	$—, —, -14.92^{+0.11}_{-0.16}$	0.90 (/H5)

where  $P_{0/1}(\mathbf{D})$  is the evidence of the noise/signal hypothesis with  $\mathbf{D}$  being the observational data.  $\phi$  is the parameters of the signal model, and  $\phi_0$  is the values making the signal hypothesis null (for instance, the values that make the amplitude of SGWB signal vanish). By employing this formula,  $\text{BF}_{10}$  can be simply expressed by the ratio of the prior to the posterior probabilities of the null hypothesis. Note that the “null” and “signal” are relative concepts depending on the parameters we focus on.

**Results.** To interpret PPTA data, we consider several typical hypotheses (labeled by  $H_n$ ) which are summarized in Table I. H0 only includes the pulsar noise. H1 is to check the existence of a strong CPL signal. H2 is to search for a DW-induced SGWB signal with the full HD correlation included. Since the origin of the CPL signal is still not clear, we further consider hypotheses H3 and H4 where we add the CPL signal as an unknown background in searching for a DW-induced SGWB signal. The difference between H3 and H4 is that H3 includes the full HD correlation while H4 only includes the off-diagonal (i.e., no-auto) HD correlation. In addition, we assume the CPL signal has an astrophysical origin, generated by SMBHBs. Analogous to H1 and H3, we get two new hypotheses, H5 and H6. In all cases, the Bayes ephemeris has been taken to include uncertainties from the solar system.

It turns out that the searches in PPTA data yield similar results for  $N_{\text{DW}} = 2$  to 6 DW networks, which is as expected since they have similar spectra as can be seen in Table S1 in the supplemental material. To be concise, in the following we present the result of  $N_{\text{DW}} = 2$  case as a benchmark while leaving the details of  $N_{\text{DW}} > 2$  results in the supplemental material.

First of all, a large Bayes factor  $\text{BF}_{10} = 10^{3.2}$  of hypothesis H1 against H0 is found in our analyses, implying the existence of a strong CPL signal, which is consistent with PTA collaborations’ work [10–12]. We then test hypothesis H2 where the CPL process is replaced by the DW signal. We derive a comparable Bayes factor of  $\text{BF}_{20} = 10^{2.1}$  when the domain wall tension,  $\sigma_{\text{DW}}$ , and the decay time,  $T_d$ , are treated as priors in

the H2. The fitting results of these parameters, at the 68% Credible Level (C.L.), are provided in Table I:

$$\sigma_{\text{DW}} \sim (29 - 414 \text{ TeV})^3, \quad T_d \sim 20 - 257 \text{ MeV}. \quad (5)$$

The corresponding 1- and 2- $\sigma$  regions of two-dimensional posterior distributions are depicted in Fig. 2. These strip regions should be interpreted as the range of domain wall parameters favored by PPTA data.

If PPTA data indeed indicates the existence of a DW network based on the H2 result, we consider the physical implications in the following discussion. In fact, GWs only carry a minor portion of DW energy, while the majority of the energy is carried by free particles decayed from the walls [4, 5]. These particles behave as matter with momentum comparable to their mass, as demonstrated by simulations [40, 41]. To prevent the matter component (composed of these free particles) from dominating the Universe too early and conflicting with BBN, a natural conclusion is that these free particles will further decay into dark radiation via their couplings with a dark sector (see, e.g., Refs. [42–45]). More details are shown in the supplemental material. This process increases the effective number of relativistic species by  $\Delta N_{\text{eff}} \equiv \rho_{\text{DR}}/\rho_{\nu}^{\text{SM}}$  where  $\rho_{\text{DR}}$  is the energy density of dark radiation, rescaled by  $\rho_{\nu}^{\text{SM}}$ , the energy density of (a single flavor) standard model neutrinos. By assuming the decay of free particles to dark radiation is instant after  $T_d$  (i.e.,  $\rho_{\text{DR}}(T_d) \simeq \rho_{\text{DW}}(T_d)$ ), we obtain

$$\Delta N_{\text{eff}} \simeq 0.077 \mathcal{A} \left[ \frac{10.75}{g_*(T_d)} \right]^{5/6} \left( \frac{\sigma_{\text{DW}}}{10^6 \text{ TeV}^3} \right) \left( \frac{100 \text{ MeV}}{T_d} \right)^2. \quad (6)$$

A more comprehensive expression for  $\Delta N_{\text{eff}}$  is presented in the supplemental material, where we also construct a succinct model that simultaneously accommodates the bias leading to wall decay and the portal facilitating the further decay of free particles into dark radiation.

It is known that  $\Delta N_{\text{eff}}$  can help resolve the Hubble tension, a  $4.1\sigma$  tension between local and early-time measurements of the Hubble parameter  $H_0$  [21, 46–51]. It has been

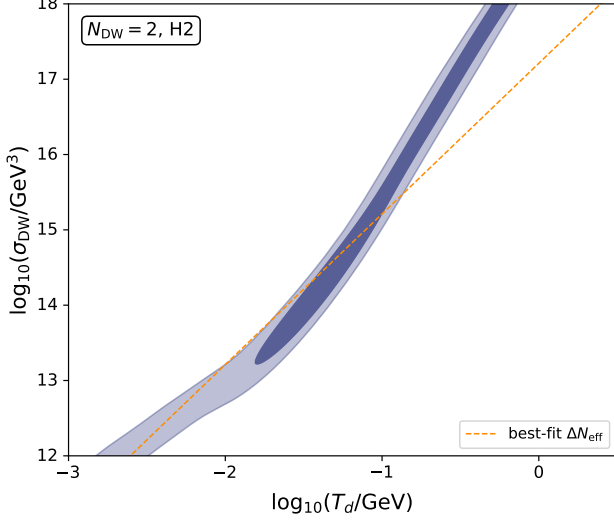


FIG. 2: Posterior distribution of  $\sigma_{\text{DW}}$  and  $T_d$  for  $N_{\text{DW}} = 2$  with the hypothesis H2 in Table I. 1 and 2- $\sigma$  regions of distribution are shown in light and dark colors. The orange dash line indicates the parameter region corresponding to the best-fit value of  $\Delta N_{\text{eff}} = 0.151$ .

shown that the existence of self-interacting dark radiation, which might be achieved in our case via the coupling with the free particles or other new dark couplings, can significantly reduce the Hubble tension to  $2.7\sigma$  with the best-fit value  $\Delta N_{\text{eff}} = 0.151$  [50, 52][72]. Then, using the above expression of  $\Delta N_{\text{eff}}$  obtained in our scenario, we search for the parameter spaces of  $\sigma_{\text{DW}}$  and  $T_d$  that give the best-fit values of  $\Delta N_{\text{eff}}$ . The results are shown in Fig. 2. We see that the best-fit line largely overlaps with the parameter space preferred by PPTA data. Therefore, both the two observations, PPTA and Hubble tension, point to the same range of DW parameters. This might be a clue to the existence of a DW network in the early Universe which decayed around the temperature  $T_d \sim 20 - 257$  MeV according to Eq. (5).

The coincidence that the same parameter space can account for the CPL and Hubble tension is very robust. It holds true for any attempts of using a DW network to explain the nano-Hertz SGWB, and it applies not only to PPTA but also to various PTA collaborations in general [10–12, 22–26]. This is easily seen as follows. As shown in Fig. 1 (or other similar plots [10–12, 22–26] showing the potential SGWB signal), the amplitude of GW spectrum should be  $\Omega_{\text{GW}} h^2 \gtrsim 10^{-9}$  in  $f \sim 10^{-9}$  to  $10^{-8}$  Hz (at least for the first a few frequency bins which are the most important ones). Combining Eq. (3) and Eq. (6), we have

$$\Omega_{\text{GW}}(f_p, T_0) h^2 \simeq 2.5 \times 10^{-9} \tilde{\epsilon} \left( \frac{\Delta N_{\text{eff}}}{0.151} \right)^2. \quad (7)$$

This relation holds independent of DW parameters. The two seemingly unrelated topics, the nano-Hertz SGWB and Hubble tension, are closely connected together via this relation. They can be simultaneously addressed by a DW network that

once existed.

On the other hand, if the strong CPL signal is not due to DWs, we can set constraints on the DW parameters. Alternatively, we specify the unknown CPL signal as generated by SMBHBs. The Bayes factor for H6 against H5 is also less than 1. Both H6 and H3 give similar results as we can see from Table I and Fig. 3. This means that assuming a specific origin (SMBHB) for the CPL signal essentially does not affect setting exclusion regions for DW parameters. As shown in Fig. 3, roughly the following parameter space in the PPTA-sensitive range is excluded:

$$\left( \frac{\sigma_{\text{DW}}}{10^7 \text{ TeV}^3} \right) \gtrsim \left( \frac{T_d}{100 \text{ MeV}} \right)^2, \text{ for } T_d \sim (1-10^{2.5}) \text{ MeV}. \quad (8)$$

It is about one order of magnitude better than the existing constraint from the requirement that DWs should not overclose the Universe [53].

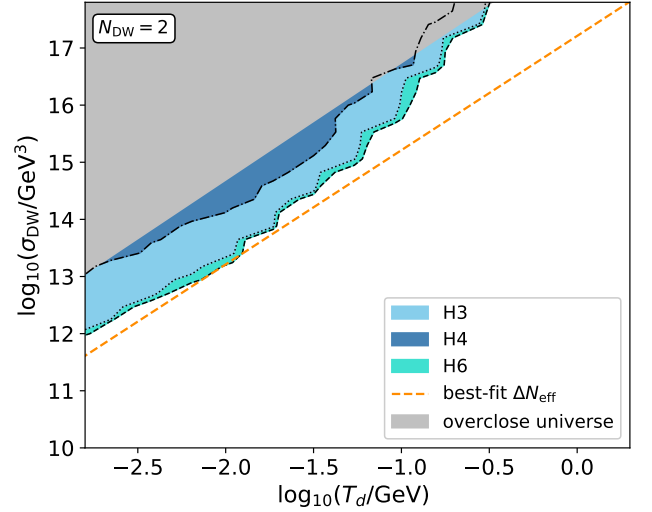


FIG. 3: 95% C.L. exclusion contour of  $\sigma_{\text{DW}}$  and  $T_d$  for  $N_{\text{DW}} = 2$  under hypotheses H3, H4 and H6 in Table I.

**Summary and discussions.** We have used PPTA DR2 to conduct a detailed search for DW networks by looking for the SGWB signal. We find a strip region of the DW parameter space can be used to explain the unknown strong CPL signal, as shown in Fig. 2 and Eq. (5). Then, we explored the cosmological implication of the scenario that free particles, as the DWs' decay product, further convert to dark radiation. Surprisingly, we find that the same parameter space of  $\sigma_{\text{DW}}$  and  $T_d$  that explains PPTA data can also significantly alleviate the Hubble tension from the reported  $4.1\sigma$  to a low level,  $2.7\sigma$ . Furthermore, such a coincidence is robust, which holds true in general for the attempts to explain the nano-Hertz SGWB using a DW network. Although we have verified this robust relation based on PPTA data, it also holds true for observations by other PTA collaborations [10–12, 22–26]. Therefore, the two seemingly unrelated subjects, nano-Hertz SGWB and Hubble

tension, turn out to be closely related within the DW framework. We conclude that a DW network in the early Universe might simultaneously account for the nano-Hertz SGWB and Hubble tension. This might represent a clue to a DW network that ever existed.

In addition, we can interpret our result in the QCD axion framework. The domain wall tension is  $\sigma_{\text{DW}} = 9.23 f_a^2 m_a$  [4]. The QCD axion mass  $m_a$  and the decay constant  $f_a$  has a fixed relation,  $\chi_a = m_a^2 f_a^2$ , where  $\chi_a$  is the topological susceptibility of QCD. One of the most recent results based on lattice simulation [54] gives that  $\chi_a \approx (75.6 \text{ MeV})^4$  for temperature below about 150 MeV. Therefore, there is a one-to-one correspondence between  $\sigma_{\text{DW}}$  and  $m_a$  and the preferred range of  $\sigma_{\text{DW}}$  in Eq. (5) can be mapped into  $m_a \sim 10^{-13} - 10^{-8} \text{ eV}$ . Although for such axions to decay into dark radiation (e.g., dark photons) may face a difficulty that the axion couplings are usually suppressed by  $f_a$ , the coupling with dark radiation could be made large enough via careful model buildings (see e.g., Refs. [45, 55]) to make a fast decay. Many terrestrial experiments aim to directly search for axions in this mass range, such as ABRACADABRA [56, 57], DM-Radio [58], SRF [59], WISPLC [60], SHAFT [61], and CASPER [62]. Searching for GW signal induced by the (axionic) DW network in PPTA data could be a cross-check and complementary to these experiments. We also explored additional hypotheses, setting the CPL process as an unknown background or from SMBHBs. Under these scenarios, we obtain the parameter space Eq. (8) ruled out at 95% C.L. Furthermore, our results indicate that networks with varying  $N_{\text{DW}}$  yield similar outcomes.

As this study concludes, we find it thrilling that the latest 15-year data from NANOGrav [22–24], EPTA’s [25] second, and CPTA’s [26] first data releases all furnish supportive evidence for the Hellings-Downs (HD) correlation. However, the HD signature cross-correlation in PPTA’s [63] third data release appears relatively weak. Despite not being able to claim the discovery of nHz gravitational waves at present, we remain hopeful. Future global Pulsar Timing Array data and enhanced large-scale cosmological defect simulations are anticipated to illuminate early universe mysteries, particularly those linked to gravitational waves and domain walls.

**Acknowledgements-** This work is supported by the National Key Research and Development Program of China under Grant No. 2020YFC2201501 and 2021YFC2203004. L.B. is supported by the National Natural Science Foundation of China (NSFC) under Grants No. 12075041 and No. 12147102. S.G. is supported by NSFC under Grant No. 12247147, the International Postdoctoral Exchange Fellowship Program, and the Boya Postdoctoral Fellowship of Peking University. C.L. is supported by the NSFC under Grants No.11963005, and No. 11603018, by Yunnan Provincial Foundation under Grants No.2016FD006 and No.2019FY003005, by Reserved Talents for Young and Middle-aged Academic and Technical Leaders in Yunnan Province Program, by Yunnan Provincial High level Talent Training Support Plan Youth Top Program, and by the NSFC

under Grant No.11847301 and by the Fundamental Research Funds for the Central Universities under Grant No. 2019CD-JDWL0005. J.S. is supported by Peking University under startup Grant No. 7101302974 and the National Natural Science Foundation of China under Grants No. 12025507, No.12150015; and is supported by the Key Research Program of Frontier Science of the Chinese Academy of Sciences (CAS) under Grants No. ZDBS-LY-7003 and CAS project for Young Scientists in Basic Research YSBR-006.

---

\* Electronic address: lgbycl@cqu.edu.cn

† Electronic address: sge@pku.edu.cn

‡ Electronic address: jshu@pku.edu.cn

- [1] T. W. Kibble, *Journal of Physics A: Mathematical and General* **9**, 1387 (1976).
- [2] W. H. Zurek, *Nature* **317**, 505 (1985).
- [3] M. Kawasaki and K. Saikawa, *Journal of Cosmology and Astroparticle Physics* **2011**, 008 (2011).
- [4] T. Hiramatsu, M. Kawasaki, K. Saikawa, and T. Sekiguchi, *Journal of Cosmology and Astroparticle Physics* **2013**, 001 (2013), ISSN 1475-7516, 1207.3166, URL <https://iopscience.iop.org/article/10.1088/1475-7516/2013/01/001>.
- [5] T. Hiramatsu, M. Kawasaki, and K. Saikawa, *Journal of Cosmology and Astroparticle Physics* **2014**, 031 (2014), ISSN 1475-7516, 1309.5001, URL <https://iopscience.iop.org/article/10.1088/1475-7516/2014/02/031>.
- [6] Y. B. Zel’dovich, I. Y. Kobzarev, and L. B. Okun, *Zh. Eksp. Teor. Fiz.* **40**, 3 (1974).
- [7] P. Sikivie, *Physical Review Letters* **48**, 1156 (1982).
- [8] G. B. Gelmini, M. Gleiser, and E. W. Kolb, *Physical Review D* **39**, 1558 (1989).
- [9] S. E. Larsson, S. Sarkar, and P. L. White, *Physical Review D* **55**, 5129 (1997).
- [10] Z. Arzoumanian et al. (NANOGrav), *Astrophys. J. Lett.* **905**, L34 (2020), 2009.04496.
- [11] B. Goncharov et al., *Astrophys. J. Lett.* **917**, L19 (2021), 2107.12112.
- [12] S. Chen et al., *Mon. Not. Roy. Astron. Soc.* **508**, 4970 (2021), 2110.13184.
- [13] R. w. Hellings and G. s. Downs, *Astrophys. J. Lett.* **265**, L39 (1983).
- [14] L. Bian, R.-G. Cai, J. Liu, X.-Y. Yang, and R. Zhou, *Phys. Rev. D* **103**, L081301 (2021), 2009.13893.
- [15] X. Xue et al., *Phys. Rev. Lett.* **127**, 251303 (2021), 2110.03096.
- [16] L. Bian, J. Shu, B. Wang, Q. Yuan, and J. Zong (2022), 2205.07293.
- [17] Z. Arzoumanian et al. (NANOGrav), *Phys. Rev. Lett.* **127**, 251302 (2021), 2104.13930.
- [18] N. Yonemaru et al., *Mon. Not. Roy. Astron. Soc.* **501**, 701 (2021), 2011.13490.
- [19] Z.-C. Chen, Y.-M. Wu, and Q.-G. Huang (2022), 2205.07194.
- [20] N. Aghanim et al. (Planck), *Astron. Astrophys.* **641**, A6 (2020), [Erratum: *Astron. Astrophys.* 652, C4 (2021)], 1807.06209.
- [21] A. G. Riess, S. Casertano, W. Yuan, L. M. Macri, and D. Scolnic, *Astrophys. J.* **876**, 85 (2019), 1903.07603.
- [22] G. Agazie et al. (NANOGrav) (2023), 2306.16213.
- [23] A. Afzal et al. (NANOGrav), *Astrophys. J. Lett.* **951** (2023), 2306.16219.

- [24] G. Agazie et al. (NANOGrav), *Astrophys. J. Lett.* **951** (2023), 2306.16217.
- [25] J. Antoniadis et al. (2023), 2306.16214.
- [26] H. Xu et al. (2023), 2306.16216.
- [27] M. Kerr, D. J. Reardon, G. Hobbs, R. M. Shannon, R. N. Manchester, S. Dai, C. J. Russell, S. Zhang, W. van Straten, S. Osłowski, et al., *Publications of the Astronomical Society of Australia* **37** (2020), URL <https://doi.org/10.1017/2Fpasa.2020.11>.
- [28] W. H. Press, B. S. Ryden, and D. N. Spergel, *The Astrophysical Journal* **347**, 590 (1989).
- [29] B. S. Ryden, W. H. Press, and D. N. Spergel, *The Astrophysical Journal* **357**, 293 (1990).
- [30] T. Garagounis and M. Hindmarsh, *Physical Review D* **68**, 103506 (2003).
- [31] A. Leite, C. Martins, and E. Shellard, *Physics Letters B* **718**, 740 (2013).
- [32] C. Caprini, M. Chala, G. C. Dorsch, M. Hindmarsh, S. J. Huber, T. Konstandin, J. Kozaczuk, G. Nardini, J. M. No, K. Rummukainen, et al., *Journal of Cosmology and Astroparticle Physics* **2020**, 024 (2020), URL <https://doi.org/10.1088/1475-7516/2020/03/024>.
- [33] C. Caprini, R. Durrer, T. Konstandin, and G. Servant, *Physical Review D* **79**, 083519 (2009).
- [34] S. M. Barr, K. Choi, and J. E. Kim, *Nucl. Phys. B* **283**, 591 (1987).
- [35] G. Hobbs, R. Edwards, and R. Manchester, *Mon. Not. Roy. Astron. Soc.* **369**, 655 (2006), [astro-ph/0603381](https://arxiv.org/abs/astro-ph/0603381).
- [36] R. T. Edwards, G. B. Hobbs, and R. N. Manchester, *Mon. Not. Roy. Astron. Soc.* **372**, 1549 (2006), [astro-ph/0607664](https://arxiv.org/abs/astro-ph/0607664).
- [37] J. Ellis and R. van Haasteren, *jellis18/ptmcmcsampler: Official release* (2017), URL <https://doi.org/10.5281/zenodo.1037579>.
- [38] B. Goncharov et al., *Mon. Not. Roy. Astron. Soc.* **502**, 478 (2021), 2010.06109.
- [39] J. M. Dickey, *The Annals of Mathematical Statistics* **42**, 204 (1971), ISSN 00034851, URL <http://www.jstor.org/stable/2958475>.
- [40] T. Hiramatsu, M. Kawasaki, K. Saikawa, and T. Sekiguchi, *Phys. Rev. D* **85**, 105020 (2012), [Erratum: *Phys. Rev. D* **86**, 089902 (2012)], 1202.5851.
- [41] M. Kawasaki, K. Saikawa, and T. Sekiguchi, *Phys. Rev. D* **91**, 065014 (2015), 1412.0789.
- [42] M. Gonzalez, M. P. Hertzberg, and F. Rompineve, *Journal of Cosmology and Astroparticle Physics* **2020**, 028 (2020).
- [43] H. Davoudiasl, *Physical Review D* **101**, 115024 (2020).
- [44] K. V. Berghaus and T. Karwal, *Physical Review D* **101**, 083537 (2020).
- [45] P. Agrawal, N. Kitajima, M. Reece, T. Sekiguchi, and F. Takahashi, *Phys. Lett. B* **801**, 135136 (2020), 1810.07188.
- [46] J. L. Bernal, L. Verde, and A. G. Riess, *JCAP* **10**, 019 (2016), 1607.05617.
- [47] N. Aghanim, Y. Akrami, M. Ashdown, J. Aumont, C. Baccigalupi, M. Ballardini, A. J. Banday, R. B. Barreiro, N. Bartolo, S. Basak, et al., *Astronomy & Astrophysics* **641**, A6 (2020), ISSN 0004-6361, URL [https://www.aanda.org/articles/aa/full\\_html/2020/09/aa33910-18/aa33910-18.html](https://www.aanda.org/articles/aa/full_html/2020/09/aa33910-18/aa33910-18.html)<https://www.aanda.org/articles/aa/abs/2020/09/aa33910-18/aa33910-18.html><https://arxiv.org/abs/1807.06209><https://dx.doi.org/10.1051/0004-6361/201833910>
- [48] A. G. Riess, S. Casertano, W. Yuan, J. B. Bowers, L. Macri, J. C. Zinn, and D. Scolnic, *The Astrophysical Journal Letters* **908**, L6 (2021).
- [49] N. Schöneberg, G. F. Abellán, A. P. Sánchez, S. J. Witte, V. Poulin, and J. Lesgourgues, *Physics Reports* **984**, 1 (2022).
- [50] E. Di Valentino, O. Mena, S. Pan, L. Visinelli, W. Yang, A. Melchiorri, D. F. Mota, A. G. Riess, and J. Silk, *Classical and Quantum Gravity* **38**, 153001 (2021), ISSN 0264-9381, URL <https://iopscience.iop.org/article/10.1088/1361-6382/ac086d><https://arxiv.org/abs/2103.01183><https://dx.doi.org/10.1088/1361-6382/ac086d>.
- [51] S. Vagnozzi, *Physical Review D* **102**, 023518 (2020), ISSN 24700029, URL <https://journals.aps.org/prd/abstract/10.1103/PhysRevD.102.023518>.
- [52] N. Blinov and G. Marques-Tavares, *Journal of Cosmology and Astroparticle Physics* **2020**, 029 (2020), ISSN 14757516, URL <https://iopscience.iop.org/article/10.1088/1475-7516/2020/09/029><https://arxiv.org/abs/10.1088/1475-7516/2020/09/029/meta>.
- [53] K. Saikawa, *Universe* **3**, 40 (2017), URL <https://doi.org/10.3390/2Funiverse3020040>.
- [54] S. Borsányi, Z. Fodor, J. Guenther, K.-H. Kampert, S. Katz, T. Kawanai, T. Kovacs, S. Mages, A. Pasztor, F. Pittler, et al., *Nature* **539**, 69 (2016).
- [55] P. Agrawal, G. Marques-Tavares, and W. Xue, *JHEP* **03**, 049 (2018), 1708.05008.
- [56] J. L. Ouellet, C. P. Salemi, J. W. Foster, R. Henning, Z. Bogorad, J. M. Conrad, J. A. Formaggio, Y. Kahn, J. Minervini, A. Radovinsky, et al., *Physical Review Letters* **122** (2019), URL <https://doi.org/10.1103/2Fphysrevlett.122.121802>.
- [57] C. P. Salemi, J. W. Foster, J. L. Ouellet, A. Gavin, K. M. Pappas, S. Cheng, K. A. Richardson, R. Henning, Y. Kahn, R. Nguyen, et al., *Physical Review Letters* **127** (2021), URL <https://doi.org/10.1103/2Fphysrevlett.127.081801>.
- [58] DMRadio Collaboration, L. Brouwer, S. Chaudhuri, H. M. Cho, J. Corbin, W. Craddock, C. S. Dawson, A. Droster, J. W. Foster, J. T. Fry, et al., *Dmradiom<sup>3</sup>: A search for the qcd axion below 1 μev* (2022), URL <https://arxiv.org/abs/2204.13781>.
- [59] A. Berlin, R. T. D’Agnolo, S. A. Ellis, and K. Zhou, *Physical Review D* **104** (2021), URL <https://doi.org/10.1103/2Fphysrevd.104.1111701>.
- [60] Z. Zhang, D. Horns, and O. Ghosh, *Physical Review D* **106** (2022), URL <https://doi.org/10.1103/2Fphysrevd.106.023003>.
- [61] A. V. Gramolin, D. Aybas, D. Johnson, J. Adam, and A. O. Sushkov, *Nature Physics* **17**, 79 (2020), URL <https://doi.org/10.1038/2Fs41567-020-1006-6>.
- [62] D. F. Jackson Kimball et al., *Springer Proc. Phys.* **245**, 105 (2020), 1711.08999.
- [63] D. J. Reardon et al. (2023), 2306.16215.
- [64] H. Murayama and J. Shu, *Phys. Lett. B* **686**, 162 (2010), 0905.1720.
- [65] S. Alam, M. Ata, S. Bailey, F. Beutler, D. Bizyaev, J. A. Blazek, A. S. Bolton, J. R. Brownstein, A. Burden, C.-H. Chuang, et al., *Monthly Notices of the Royal Astronomical Society* **470**, 2617 (2017).
- [66] A. J. Ross, L. Samushia, C. Howlett, W. J. Percival, A. Burden, and M. Manera, *Monthly Notices of the Royal Astronomical Society* **449**, 835 (2015).
- [67] F. Beutler, C. Blake, M. Colless, D. H. Jones, L. Staveley-Smith, L. Campbell, Q. Parker, W. Saunders, and F. Watson, *Monthly Notices of the Royal Astronomical Society* **416**, 3017 (2011).

- [68] D. M. Scolnic, D. Jones, A. Rest, Y. Pan, R. Chornock, R. Foley, M. Huber, R. Kessler, G. Narayan, A. Riess, et al., *The Astrophysical Journal* **859**, 101 (2018).
- [69] For topological defects formation during the phase transition through Kibble-Zurek mechanism and its connection with dark matter, see Ref.[64].
- [70] <https://github.com/nanograv/enterprise>
- [71] [https://github.com/nanograv/enterprise\\_extensions](https://github.com/nanograv/enterprise_extensions)
- [72] Different choices of datasets can reduce the Hubble tension to different levels. Here, the  $2.7\sigma$  tension is obtained by fitting to the dataset of *Planck 2018 + CMB lensing* [47] with a freely-varying self-interacting  $\Delta N_{\text{eff}}$ . The tension would be reduced to  $2.9\sigma$  [52] with *BAO* data [65–67] included and  $3.2\sigma$  [49] with *Pantheon* data [68] further included.



# Supplemental material for Searching for Domain Wall Network: A Dual Solution for Gravitational Waves and Hubble Tension?

## I. GW SPECTRA

Refs. [1, 2] have numerically simulated in detail the generation of GWs by DW networks with different  $N_{\text{DW}}$  based on QCD axion model and  $\lambda\phi^4$  model. But their result is quite general as the shape of the DW-induced GWs is primarily model-independent. Here, we directly fit for the slope-power  $P$  from the simulation result shown as Figure 6 in [1]. The fitted power values are summarized in Table S1. For the different  $N_{\text{dw}}$ , the complete GW spectra can be parameterized as  $\Omega_{\text{GW}}(f, T_0)h^2 = \Omega_{\text{GW}}(f_p, T_0)h^2 \times (f/f_p)^n$  where  $n = 3$  (and  $n = P$ ) for  $f < f_p$  (and  $f > f_p$ ).

Table S1. Fitted power value  $P$  for  $f > f_p$ .

$N_{\text{DW}}$	2	3	4	5	6
$P$	-1.077	-0.972	-0.887	-0.807	-0.731

$n = P$  for  $f > f_p$ .

## II. PARAMETERS SUMMARY

The prior distributions and descriptions of the parameters of DW, PTA noise models, and SGWB model are summarized in Table S2.

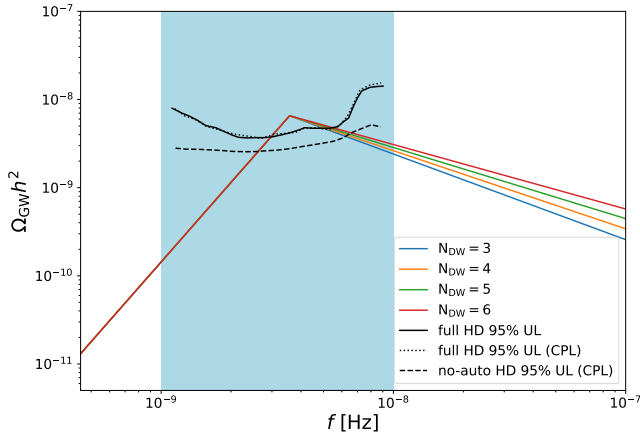


Figure S1. Same as Fig.1 in the main text, but for  $N_{\text{DW}} \geq 2$  cases. Also, the parameters are fixed at  $(\log_{10} \sigma_{\text{DW}}/\text{GeV}^3, \log_{10} T_d/\text{GeV}) = (14.5, -1.5)$  for illustrative purpose.

## III. RESULTS FROM OTHER HYPOTHESES

DWs with  $N_{\text{DW}} > 2$  are also considered in our model, and we here list the search results for  $N_{\text{DW}} = 3, 4, 5$  and 6. First,

we show the GW spectra corresponding to these  $N_{\text{DW}}$  values along with the free-spectra search of the SGWB amplitude in Fig. S1. Then, for each  $N_{\text{DW}}$ , we repeat the procedure of data analysis as done for the  $N_{\text{DW}} = 2$  case. We summarize the detailed components of every hypothesis, the  $1-\sigma$  regions of parameters, and the Bayes factor between different hypotheses in Table S3. Figs. S2-S5 show the posterior distributions of the parameters in different hypotheses described in the table, corresponding to the cases of the  $N_{\text{DW}}$  values of 3 and 6. As can be seen, DW networks with  $N_{\text{DW}} > 2$  can also offer a good explanation for the strong CPL process, with the Bayes factors of H2 ranging from  $10^{1.2}$  to  $10^{1.8}$  against the null hypothesis H0. Moreover, results similar to the  $N_{\text{DW}} = 2$  case also arise when we include the CPL process as a background component, no matter whether we maintain the auto-correlation between the pulsars or consider the CPL process as an astrophysical source from the SMBHB. The Bayes factors are all distributed around 1, meaning a disfavoured evidence for H3/4/6 against H1. It might be helpful to distinguish between DW networks with different  $N_{\text{DW}}$  values, with more observation data coming in the near future, but we can only give the constraints on the parameters for now. The  $1-\sigma$  C.L. limits of these parameters are all listed in Table S3.

To be complementary, we also reproduce the strong CPL signal using hypothesis H1. The CPL spectrum used in this paper is represented by

$$S(f) = \frac{A_{\text{CPL}}}{12\pi^2} \left( \frac{f}{\text{yr}^{-1}} \right)^{-\gamma_{\text{CPL}}} \text{yr}^3. \quad (\text{S1})$$

We obtain a  $1-\sigma$  region for the amplitude and spectra index:  $\log_{10} A_{\text{CPL}} = -14.48^{+0.62}_{-0.64}$  and  $\gamma_{\text{CPL}} = 3.34^{+1.37}_{-1.53}$  with the Bayes factor of  $\text{BF} = 10^{3.2}$ . Then we made a trial to explain the CPL signal by using the solely SMBHB process (H5), and it turned out to be a good explanation with a large Bayes factor,  $\text{BF} = 10^{3.3}$ , against the null hypothesis H0. The posterior distribution for  $\log_{10} A_{\text{SMBHB}}$  is shown in Fig. S6. Then we also give the  $1-\sigma$  region of the amplitude:  $\log_{10} A_{\text{SMBHB}} = -14.89^{+0.10}_{-0.12}$ . Note that the SGWB spectrum from the SMBHB used in this work is given by:

$$S(f) = \frac{A_{\text{SMBHB}}}{12\pi^2} \left( \frac{f}{\text{yr}^{-1}} \right)^{-\gamma_{\text{SMBHB}}} \text{yr}^3. \quad (\text{S2})$$

In this case,  $\gamma_{\text{SMBHB}}$  is fixed at  $13/3$ , and  $A_{\text{SMBHB}}$  is assumed to take the prior distribution of  $\log\text{-U} [-18, -14]$ .

We notice that Ref. [3] made a similar search by using both the NANOGrav 12.5 years datasets [4] (NG12) and the International PTA Data Release 2 datasets [5] (IPTA DR2). Note that the PPTA DR2 we used in this work is independent of IPTA DR2. Besides, we also differ from them in the search strategies. The SGWB spectra used here are directly interpreted from the result of the large field simulation [1], and we extract out the corresponding spectra for every single value



Table S2. Parameters and their prior distribution in data analysis. U and log-U stand for the uniform and log-uniform distribution.

parameter	Description	Prior	Comments
Noise parameters( $\vartheta$ )			
EFAC	White-noise modifier per backend	U [0, 10]	Fixed for setting limits
EQUAD	Quadratic white noise per backend	log-U [-10, -5]	Fixed for setting limits
ECORR	Correlated-ToAs white noise per backend	log-U [-10, -5]	Fixed for setting limits
$A_{\text{SN}}$	Spin-noise amplitude	log-U [-20, -6] (search) U [ $10^{-20}$ , $10^{-6}$ ] (limit)	One parameter per pulsar
$\gamma_{\text{SN}}$	Spin-noise spectral index	U [0, 10]	One parameter per pulsar
$A_{\text{DM}}$	DM-noise amplitude	log-U [-20, -6] (search) U [ $10^{-20}$ , $10^{-6}$ ] (limit)	One parameter per pulsar
$\gamma_{\text{DM}}$	DM-noise spectral index	U [0, 10]	One parameter per pulsar
$A_{\text{BAND}}$	Band-noise amplitude	log-U [-20, -6] (search) U [ $10^{-20}$ , $10^{-6}$ ] (limit)	One parameter partial pulsars
$\gamma_{\text{BAND}}$	Band-noise spectral index One parameter per pulsar	U [0, 10]	One parameter partial pulsars
$A_{\text{CHROM}}$	Chromatic-noise amplitude	log-U [-20, -6] (search) U [ $10^{-20}$ , $10^{-6}$ ] (limit)	One parameter partial pulsars
$\gamma_{\text{CHROM}}$	Chromatic-noise spectral index	U [0, 10]	One parameter partial pulsars
$n_{\text{CHROM}}$	Index of chromatic effects	U [0, 6]	Fixed for single pulsar
$A_{\text{CPL}}$	CPL process amplitude	log-U [-18, -11] (search) U [ $10^{-18}$ , $10^{-11}$ ] (limit)	One parameter per PTA
$\gamma_{\text{CPL}}$	CPL process power index	U [0, 7]	One parameter per PTA
DW networks signal parameters ( $\psi$ )			
$N_{\text{DW}}$	DW number	[2, 3, 4, 5, 6] (fixed for each search)	One parameter per PTA
$\sigma_{\text{DW}}[\text{GeV}^3]$	Wall tension	log-U [10, 18] (search) U [ $10^{10}$ , $10^{18}$ ] (limit)	One parameter per PTA
$T_d[\text{GeV}]$	Decay temperature	log-U [-3, 5] (search) U [ $10^{-3}$ , $10^5$ ] (limit)	One parameter per PTA
BayesEphem parameters ( $\phi$ )			
$z_{\text{drift}}$	Drift-rate of Earth's orbit about ecliptic z-axis	U[- $10^{-9}$ , $10^{-9}$ ] rad yr $^{-1}$	One parameter per PTA
$\Delta M_{\text{Jupiter}}$	Perturbation of Jupiter's mass	$N(0, 1.5 \times 10^{-11}) M_{\odot}$	One parameter per PTA
$\Delta M_{\text{Saturn}}$	Perturbation of Saturn's mass	$N(0, 8.2 \times 10^{-12}) M_{\odot}$	One parameter per PTA
$\Delta M_{\text{Uranus}}$	Perturbation of Uranus' mass	$N(0, 5.7 \times 10^{-11}) M_{\odot}$	One parameter per PTA
$\Delta M_{\text{Neptune}}$	Perturbation of Neptune's mass	$N(0, 7.9 \times 10^{-11}) M_{\odot}$	One parameter per PTA
$PCA_i$	Principal components of Jupiter's orbit	U [-0.05, 0.05]	One parameter per PTA

of  $N_{\text{DW}}$  instead of treating it as a continuous parameter. By doing this, we can remove the uncertainty of one additional parameter in searching. The searches in PPTA data yield similar results for  $N_{\text{DW}} = 2$  to 6 DW networks. This is as expected because they have similar GW spectra as can be seen in Table S1. To be concise, we have shown the  $N_{\text{DW}} = 2$  case as a benchmark in the main text, while leaving the details of  $N_{\text{DW}} > 2$  results in the Supplemental Material as shown above. We have made a more thorough search including a) a direct search for the SGWB in the data with only white and red noises included, which yields the best-fit parameter values of DW; b) include or not include the auto-correlation between the pulsar pairs while taking the CPL as a systematic error, since the source of CPL still remains unknown; c) joint search for SGWB from the SMBHB and DW. As seen in [3], they only focused on parts a) and c). Besides, they set the HD overlap

reduction function  $\Gamma_{ab} = 1$  to simplify the computation while we adopt the strict formula to be conservative

#### IV. THE DOMAIN WALL NETWORKS AND $\Delta N_{\text{eff}}$

DW network can release its energy into two forms: GWs and free particles (i.e., axions or scalar particles) that build the walls, with the quantitative relation  $\rho_{\text{GW}}/\rho_{\text{DW}} = 3/(8\pi) \cdot \epsilon \cdot \rho_{\text{DW}}/\rho_c$ . Taking the typical values  $\sigma_{\text{DM}} = 10^{14} \text{ GeV}^3$  and  $T_d \sim 20 \text{ MeV}$ , we get  $\rho_{\text{GW}}/\rho_c \sim 10^{-5}$  and  $\rho_{\text{DW}}/\rho_c \sim 10^{-2}$  at  $T_d$ , which means that most of the energy is released into free particles. Furthermore, simulations show that those particles behave as cold matter with momentum comparable to the mass [1]. Consequently, for the parameter space we are interested in, such cold matter can dominate the Universe too

early, which contradicts cosmological observations. Here, we consider one simple solution: those free particles can further decay into dark relativistic species (i.e., dark radiation, DR) via their couplings with a dark sector [6–8]. In this picture, free particles decay and inject energy into the dark radiation. It causes an increase in the effective number of relativistic species,  $\Delta N_{\text{eff}} \equiv \rho_{\text{DR}}/\rho_{\nu}^{\text{SM}}$  where  $\rho_{\nu}^{\text{SM}}$  is the energy density of (a single flavor) standard model neutrinos. A model-independent calculation shows that our scenario gives

$$\Delta N_{\text{eff}} \simeq \left(\frac{4}{11}\right)^{-\frac{4}{3}} \cdot \frac{4}{7} \cdot \frac{\rho_{\text{DW}}(T_d)}{\rho_c(T_d)} g_{*s}^{4/3}(T) g_{*s}^{-1/3}(T_d) \cdot F(\Gamma), \quad (\text{S3})$$

with  $F(\Gamma) = \int_{t_d}^t \frac{a(t')}{a(t_d)} e^{-\Gamma(t'-t_d)} \Gamma dt'.$

$g_{*s}$  is the effective degree of freedom for entropy.  $\Gamma$  is the decay rate from free particles to dark radiation. We require a large  $\Gamma$  to complete the decay before the BBN epoch  $\sim 1$  MeV to avoid the potential violation of BBN observations. If  $\Gamma$  is sufficiently large ( $\Gamma \gg t_d^{-1}$ ),  $F(\Gamma) \simeq 1$  which returns to the case discussed in Ref. [3]. Furthermore, we expect that if the decay is not instant, in addition to alleviating the Hubble tension with the dark radiation, the residual free particles can also serve as dark matter. One can find various examples of such no-instant decay processes, for instance, in Ref. [9]). This issue is worthy of further study. Contrastingly, the network of

long cosmic strings in the scaling regime can not alleviate the Hubble tension. The maximal contribution to  $\Delta N_{\text{eff}}$  from its decay is less than  $10^{-6}$ , adhering to the limit established by LIGO’s observations, where  $\Omega_{\text{gw}} h^2 < 10^{-7}$  [10]. This underscores the significant role of the DW network in alleviating the Hubble tension.

Finally, we build a simple model as an example to allow free particles to further decay into dark radiation. We consider a potential  $V(\phi) = \lambda/4(\phi^2 - \eta^2)^2$  which can form a  $Z_2$  domain wall network.  $\phi$  represents the scalar field that constitutes the wall,  $\eta$  denotes the energy scale of spontaneous  $Z_2$  symmetry breaking, and the domain wall tension,  $\sigma_{\text{DW}}$ , is given by  $\sigma_{\text{DW}} = 2\sqrt{2}\lambda\eta^3/3$ . We suppose the  $Z_2$  symmetry is explicitly broken by the term

$$V_{\text{breaking}} = \kappa\eta \cdot \phi\chi^2. \quad (\text{S4})$$

Here,  $\chi$  signifies an ultralight scalar field that can be approximated as a classical field with the mean-field value  $\langle\chi\rangle$ . This coupling term Eq. (S4) fulfills a dual role. Firstly, it can induce wall decay through the bias potential  $\Delta V = 2\kappa\eta^2 \langle\chi\rangle^2$ , which equates to the energy density  $\sigma_{\text{DW}}/t$  during the DW decay. Secondly, via this coupling term, the free particles resulting from wall decay will further rapidly decay into ultralight  $\chi$  particles, which behave as dark radiation.

- 
- [1] T. Hiramatsu, M. Kawasaki, K. Saikawa, and T. Sekiguchi, *Journal of Cosmology and Astroparticle Physics* **2013**, 001 (2013), ISSN 1475-7516, 1207.3166, URL <https://iopscience.iop.org/article/10.1088/1475-7516/2013/01/001>.
- [2] T. Hiramatsu, M. Kawasaki, and K. Saikawa, *Journal of Cosmology and Astroparticle Physics* **2014**, 031 (2014), ISSN 1475-7516, 1309.5001, URL <https://iopscience.iop.org/article/10.1088/1475-7516/2014/02/031>.
- [3] R. Z. Ferreira, A. Notari, O. Pujolas, and F. Rompineve (2022), 2204.04228.
- [4] M. F. Alam, Z. Arzoumanian, P. T. Baker, H. Blumer, K. E. Bohler, A. Brazier, P. R. Brook, S. Burke-Spolaor, K. Caballero, R. S. Camuccio, et al., *The Astrophysical Journal Supplement Series* **252**, 4 (2020), URL <https://doi.org/10.3847/2F1538-4365%2Fabc6a0>.
- [5] B. B. P. Perera, M. E. DeCesar, P. B. Demorest, M. Kerr, L. Lentati, D. J. Nice, S. Osłowski, S. M. Ransom, M. J. Keith, Z. Arzoumanian, et al., *Monthly Notices of the Royal Astronomical Society* **490**, 4666 (2019), URL <https://doi.org/10.1093%2Fmnras%2Fstz2857>.
- [6] M. Gonzalez, M. P. Hertzberg, and F. Rompineve, *Journal of Cosmology and Astroparticle Physics* **2020**, 028 (2020).
- [7] H. Davoudiasl, *Physical Review D* **101**, 115024 (2020).
- [8] K. V. Berghaus and T. Karwal, *Physical Review D* **101**, 083537 (2020).
- [9] C. Li, *Phys. Rev. D* **102**, 123530 (2020), 2008.10264.
- [10] J. A. Dror, T. Hiramatsu, K. Kohri, H. Murayama, and G. White, *Phys. Rev. Lett.* **124**, 041804 (2020), 1908.03227.

Table S3. Description of the hypotheses, Bayes factors, and parameters estimation of  $N_{\text{DW}} > 2$ .

Hypothesis	Pulsar Noise	CPL	SMBHB	DW Spectra	Parameter Estimation (68% C.L.)		
					$\log_{10} T_d/\text{GeV}, \log_{10} \sigma_{\text{DW}}/\text{GeV}^3$	$A_{\text{CPL}}, \gamma_{\text{CPL}}, A_{\text{SMBHB}}(T_d)$	Bayes Factors ( $T_d$ )
H0	✓				—	—	—
H1	✓	✓			—	$-14.48^{+0.62}_{-0.64}, 3.34^{+1.37}_{-1.53}, —$	$10^{3.2} (/H0)$
H2	$N_{\text{DW}} = 3$	✓		✓(full HD)	$-1.34^{+0.69}_{-0.56}, 14.31^{+2.29}_{-1.35}$	—	$10^{1.8} (/H0)$
	$N_{\text{DW}} = 4$	✓		✓(full HD)	$-1.27^{+0.67}_{-0.54}, 14.38^{+2.31}_{-1.44}$	—	$10^{1.5} (/H0)$
	$N_{\text{DW}} = 5$	✓		✓(full HD)	$-1.34^{+0.70}_{-0.65}, 14.29^{+2.28}_{-1.65}$	—	$10^{1.2} (/H0)$
	$N_{\text{DW}} = 6$	✓		✓(full HD)	$-1.32^{+0.69}_{-0.69}, 14.30^{+2.29}_{-1.67}$	—	$10^{1.2} (/H0)$
H3	$N_{\text{DW}} = 3$	✓	✓	✓(full HD)	$> -1.31, < 16.50$	$-14.63^{+0.67}_{-0.97}, 3.34^{+1.49}_{-1.67}, —$	$0.98 (/H1)$
	$N_{\text{DW}} = 4$	✓	✓	✓(full HD)	$> -1.22, < 16.51$	$-14.67^{+0.66}_{-0.99}, 3.41^{+1.47}_{-1.65}, —$	$1.00 (/H1)$
	$N_{\text{DW}} = 5$	✓	✓	✓(full HD)	$> -1.28, < 16.47$	$-14.63^{+0.65}_{-0.89}, 3.38^{+1.43}_{-1.62}, —$	$0.97 (/H1)$
	$N_{\text{DW}} = 6$	✓	✓	✓(full HD)	$> -1.30, < 16.53$	$-14.58^{+0.68}_{-1.09}, 3.18^{+1.57}_{-1.65}, —$	$0.97 (/H1)$
H4	$N_{\text{DW}} = 3$	✓	✓	✓(no-auto HD)	$> -0.95, < 16.52$	$-11.11^{+0.08}_{-0.13}, 0.34^{+0.37}_{-0.21}, —$	$0.89 (/H1)$
	$N_{\text{DW}} = 4$	✓	✓	✓(no-auto HD)	$> -0.97, < 16.46$	$-11.07^{+0.05}_{-0.09}, 0.65^{+0.27}_{-0.18}, —$	$0.89 (/H1)$
	$N_{\text{DW}} = 5$	✓	✓	✓(no-auto HD)	$> -0.23, < 16.31$	$-13.12^{+0.13}_{-0.13}, 3.62^{+0.32}_{-0.28}, —$	$0.93 (/H1)$
	$N_{\text{DW}} = 6$	✓	✓	✓(no-auto HD)	$> -1.06, < 16.40$	$-13.08^{+0.17}_{-0.16}, 3.87^{+0.38}_{-0.38}, —$	$0.89 (/H1)$
H5	✓		✓		—	$—, —, -14.89^{+0.10}_{-0.12}$	$10^{3.3} (/H0)$
H6	$N_{\text{DW}} = 3$	✓	✓	✓(full HD)	$> -1.00, < 16.47$	$—, —, -14.92^{+0.11}_{-0.16}$	$0.91 (/H5)$
	$N_{\text{DW}} = 4$	✓	✓	✓(full HD)	$> -1.07, < 16.46$	$—, —, -14.92^{+0.11}_{-0.16}$	$0.90 (/H5)$
	$N_{\text{DW}} = 5$	✓	✓	✓(full HD)	$> -1.05, < 16.44$	$—, —, -14.93^{+0.12}_{-0.16}$	$0.91 (/H5)$
	$N_{\text{DW}} = 6$	✓	✓	✓(full HD)	$> -1.11, < 16.46$	$—, —, -14.93^{+0.12}_{-0.18}$	$0.92 (/H5)$

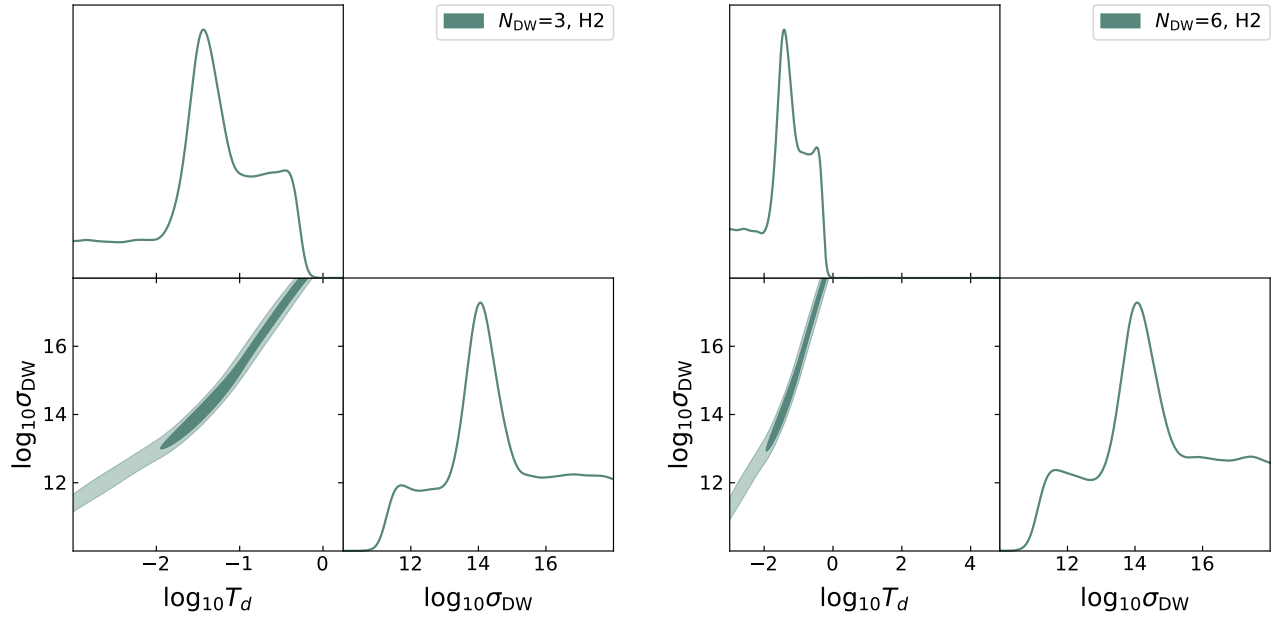


Figure S2. Posterior distribution of the decay temperature  $\log_{10}(T_d/\text{GeV})$  and the wall tension  $\log_{10}(\sigma_{\text{DW}}/\text{GeV}^3)$  with  $N_{\text{DW}} = 3$  and 6 for hypothesis H2 in Table S3.

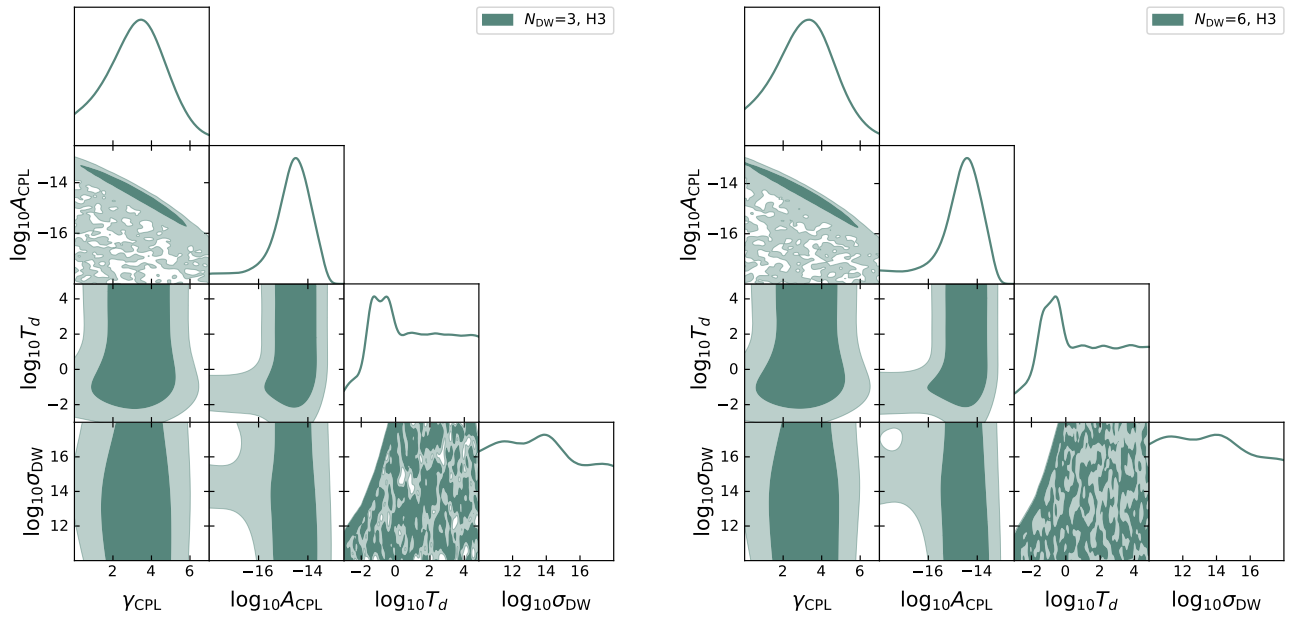


Figure S3. Posterior distribution of the decay temperature  $\log_{10}(T_d/\text{GeV})$  and the wall tension  $\log_{10}(\sigma_{\text{DW}}/\text{GeV}^3)$  with  $N_{\text{DW}} = 3$  and 6 for hypothesis H3 in Table S3.

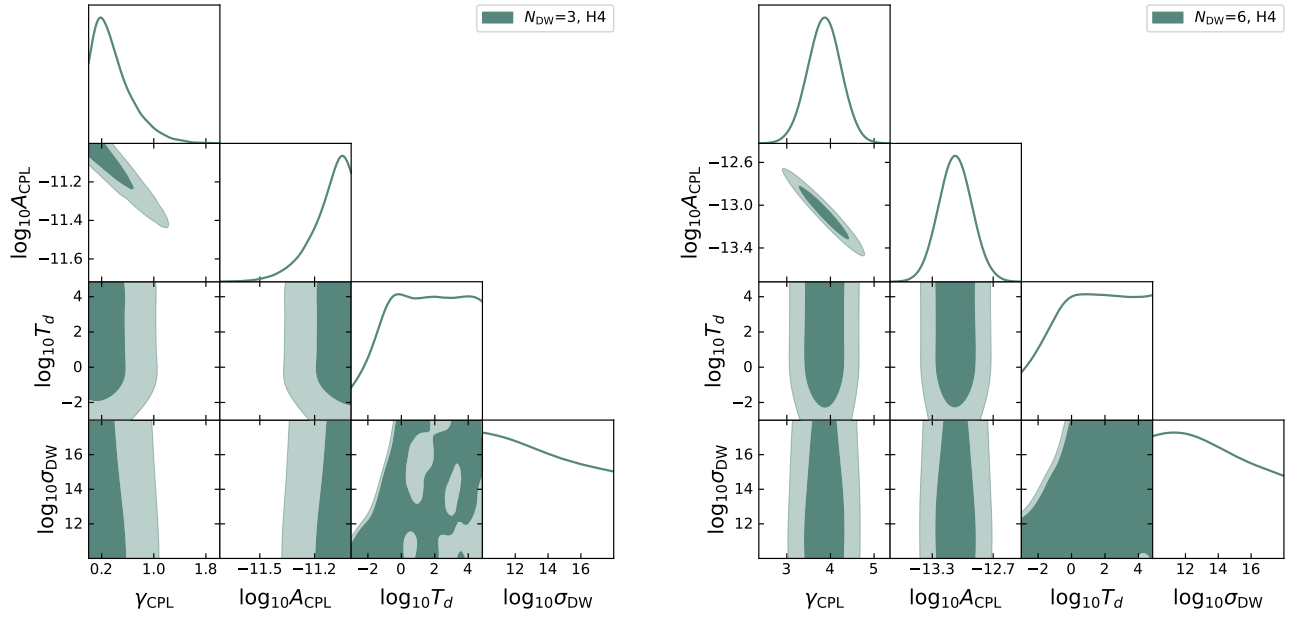


Figure S4. Posterior distribution of the decay temperature  $\log_{10}(T_d/\text{GeV})$  and the wall tension  $\log_{10}(\sigma_{\text{DW}}/\text{GeV}^3)$  with  $N_{\text{DW}} = 3$  and 6 for hypothesis H4 in Table S3.

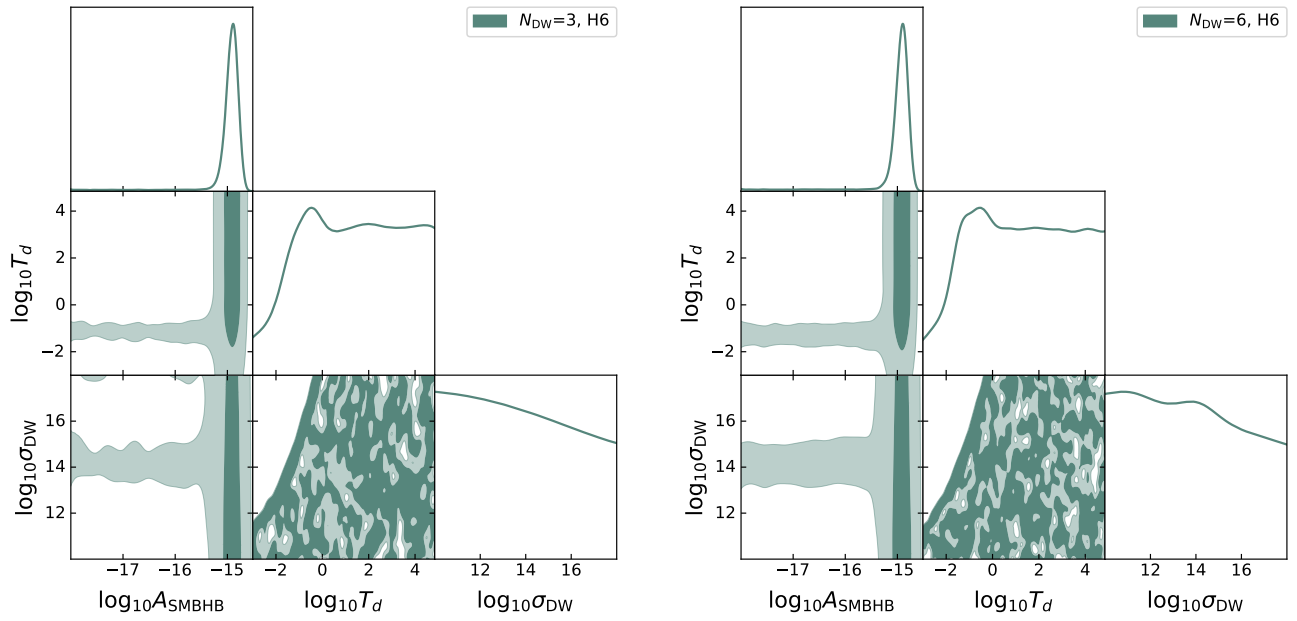


Figure S5. Posterior distribution of the decay temperature  $\log_{10}(T_d/\text{GeV})$  and the wall tension  $\log_{10}(\sigma_{\text{DW}}/\text{GeV}^3)$  with  $N_{\text{DW}} = 3$  and 6 for hypothesis H6 in Table S3.

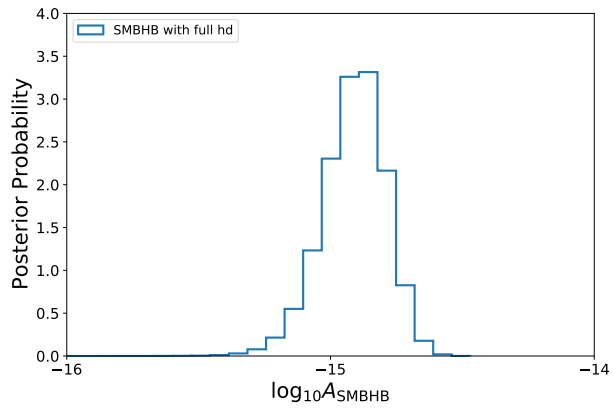


Figure S6. Posterior distribution of  $A_{\text{SMBHB}}$  of the H5 case in the TableS3.